Solvent Effects on the Energetics of Intermolecular Charge-Transfer Reactions

Erin O'Driscoll, John D. Simon,*,† and Kevin S. Peters*

Contribution from the Department of Chemistry, University of Colorado, Boulder, Colorado 80309. *Received February 5, 1990*

Abstract: Picosecond absorption spectroscopy is used to examine the intermolecular electron-transfer reaction between the *trans*-stilbene radical cation and a series of olefin radical anions in polar solvents. Laser excitation of a ground-state complex between *trans*-stilbene and electron-deficient olefins selectively generates the contact ion pair within the time resolution of the experiment. By monitoring the time-dependent absorption of the *trans*-stilbene radical cation, the dynamics of electron back-transfer and ion-pair separation are studied. The rate of electron back-transfer is found to be temperature independent in the series of polar aprotic solvents over the temperature range from −8 °C to +80 °C. However, a linear correlation is observed between the charge-transfer rate and solvent polarity. With this result, the temperature data are interpreted in terms of solvent polarity effects on the activation energy for charge transfer. Once the rates are corrected for variation of solvent polarity, activation parameters are determined and the contributions of solvation and intramolecular modes to the reorganizational energy are evaluated. The dynamics of ion-pair separation are also briefly discussed.

Introduction

Prompted by advances in our understanding of liquid-state dynamics[1-5] there has been considerable interest in elucidating the role of solvent dynamics in electron-transfer reactions.[1,6-11] Electron transfer is one of the most basic chemical reactions and occurs in a wide variety of chemical and biological systems. When such reactions are examined in solution, it is useful to think about solvent effects on the reaction in terms of both static and dynamic effects. Static effects include all changes in the potential energy surface of the reaction that are induced by properties of the solvent and would include the dependence of the free energies of reactants and products that are associated with changes in dielectric properties of the medium. In reactions where there is substantial charge development in the activated complex (or in the formation of the product), large rate accelerations or decelerations have been observed with increasing solvent polarity.[12,13]

In addition to these effects, there has been considerable recent interest in examining the role of solvent dynamics in determining electron-transfer reaction rates. These efforts are aimed at exploring the coupling of the reaction surface to fluctuations in the surrounding fluid and can either activate or deactivate the chemical reaction as well as induce multiple crossings of the reaction trajectory at the top of the reaction barrier.[14-16]

In general, the rate constant of an electron-transfer reaction (k_{et}) is expressed as

$$k_{et} = A \exp\left(\frac{-\Delta G^{\ddagger}}{RT}\right) \quad (1)$$

Static solvent effects enter into this expression through the activation energy ($\Delta G^{\ddagger}$), while dynamic solvation is incorporated in the frequency factor (A). By use of Marcus theory, the activation energy can be related to the exoergicity of the reaction (ΔG_0) and the reorganization energy (λ)[17]

$$\Delta G^{\ddagger} = \frac{(\Delta G_0 + \lambda)^2}{4\lambda} \quad (2)$$

Experimental studies of electron-transfer processes often focus on the validity of this free energy relationship and determination of the magnitude of λ. This free energy relationship predicts a parabolic dependence of the reaction rate on exoergicity, with a maximum rate expected when $\Delta G_0 = -\lambda$. For $-\Delta G_0 > \lambda$, the rate is predicted to decrease with increasing exoergicity. This region, commonly referred to as the Marcus inverted region, has been the subject of several studies.[18-22] In general, this free energy relationship describes the behavior of a wide variety of experimental systems. Most attempts at mapping out the entire Marcus curve have involved changing either the donor or the acceptor to affect a change in the ΔG_0 of the reaction. While this is an efficient way to alter the overall free energy, many other important factors in determining the rate of electron transfer are also affected, including, but not limited to, the prefactor, the distance of electron transfer, the electronic overlap, and the internal reorganization factor. The free energy can also be changed by simply varying the solvent. In the present study, two sets of experiments are carried out in which the reaction exoergicity is altered by changing either the solvent or the electron acceptor. Taken independently, these two approaches to varying the reaction exoergicity result in different interpretations accounting for the effect of energetics on the reaction rate constant. Our results clearly point out that several different types of experiments must be performed in order to accurately evaluate the role of exoergicity on reaction rate constants.

† NSF Presidential Young Investigator 1985-1990, Alfred P. Sloan Fellow 1988-1990, Camile and Henry Dreyfus Teacher Scholar 1990-1995. Permanent address: Department of Chemistry, University of California at San Diego, La Jolla, CA 92093

(1) Maroncelli, M.; MacInnis, J.; Fleming, G. R. *Science (Washington, D.C.)* **1989**, *243*, 164.
(2) Simon, J. D. *Acc. Chem. Res.* **1988**, *21*, 128.
(3) Bagchi, B. *Annu. Rev. Phys. Chem.* **1989**, *40*, 115.
(4) Barbara, P. F.; Jarzeba, W. *Adv. Photochem.* **1990**, in press.
(5) Simon, J. D.; Hynes, J. T. *Chem. Rev.* **1991**, manuscript in preparation.
(6) Heitele, H.; Finckh, P.; Weeren, S.; Pollinger, F.; Michel-Beyerle, M. E. *J. Phys. Chem.* **1989**, *93*, 5173.
(7) Heitele, H.; Michel-Beyerle, M. E. *Chem. Phys. Lett.* **1987**, *138*, 237.
(8) McManis, G. E.; Weaver, M. J. *J. Chem. Phys.* **1989**, *90*, 912.
(9) Mikkelsen, K. V.; Ratner, M. A. *Int. J. Quantum Chem., Quantum Chem. Symp.* **1988**, *22*, 707.
(10) Su, S-G.; Simon, J. D. *J. Chem. Phys.* **1988**, *89*, 908.
(11) Kahlow, M. A.; Kang, T. J.; Barbara, P. F. *J. Phys. Chem.* **1987**, *91*, 6452.
(12) Alfassi, Z. B.; Mosseri, S.; Neta, P. *J. Phys. Chem.* **1987**, *91*, 3383.
(13) Mataga, N.; Kanda, Y.; Okada, T. *J. Phys. Chem.* **1986**, *90*, 3880.
(14) Grote, R. F.; Hynes, J. T. *J. Chem. Phys.* **1980**, *73*, 2715.
(15) Zichi, D. A.; Ciccotti, G.; Hynes, J. T.; Ferrario, M. *J. Phys. Chem.* **1989**, *93*, 6261.
(16) Bader, J. S.; Chandler, D. *Chem. Phys. Lett.* **1989**, *157*, 501.
(17) Marcus, R. A.; Siders, P. *J. Phys. Chem.* **1982**, *86*, 622.
(18) Closs, G. L.; Calcaterra, L. T.; Green, N. J.; Penfield, K. W.; Miller J. R. *J. Phys. Chem.* **1986**, *96*, 3673.
(19) Gould, I. R.; Moser, J. E.; Armitage, B. *J. Am. Chem. Soc.* **1989**, *111*, 1917.
(20) Gould, I. R.; Moser, J. E.; Moody, R.; Armitage, B.; Farid, S. *Science* (Washington, D.C.) **1989**, *246*, 33.
(21) Mataga, N.; Ohno, T.; Yoshimura, A. *J. Phys. Chem.* **1986**, *90*, 3295.
(22) Mataga, N.; Kakitani, T. *J. Phys. Chem.* **1985**, *89*, 8.

0002-7863/90/1512-7091$02.50/0

In the last decade, there has been interest in determining how solvent effects are expressed in the frequency factor (A). Using a Debye dielectric continuum description of the solvent, one predicts that, in the strong coupling limit, A will correlate inversely with the longitudinal relaxation time of the liquid, τ_L.[8,23-35] However, when exploring the importance of solvent dynamics in determining the rate constant, one must have an accurate measure of the relaxation time of the surrounding fluid. Recently, the use of τ_L as a measure of solvent relaxation has come under considerable scrutiny.[1-5] This has been prompted by a large experimental and theoretical effort to determine solvent relaxation dynamics. Experimental measurements of the time-resolved Stokes shift of a dissolved polar probe molecule have provided information concerning the microscopic relaxation dynamics of polar fluids.[1-5,36-38]

This paper investigates the role of solvent dynamics and statics on an intermolecular electron-transfer reaction between the two radical ions of a photogenerated contact ion pair. The majority of experimental studies that address the details of solvent static and dynamic effects on chemical reactions have focused on intramolecular systems. Both rigid molecular systems[18] as well as molecules that undergo internal twisting[39] have been examined. These latter systems have been of interest as they provide well-defined systems for evaluating the importance of solvation and torsional motion in determining the total reorganization energy and the reaction rate constant.[10] However, it is important to consider that both dynamic and static effects can have a tremendous impact on determining the reaction rate. In studies of the twisted intramolecular charge-transfer reaction of (*N*,*N*-dimethylamino)benzonitrile in a series of nitrile solvents[40,41] and bis[4,4′-bis(dialkylamino)phenyl]sulfone in a series of alcohol solvents,[42] it was demonstrated that the changes in polarity that occurred in varying the solvent effectively masked the effect of solvent viscosity on the reaction rate. These studies point out that in reactions that involve substantial change in charge distribution of the reacting system changes in the dielectric properties of the liquid can significantly alter the potential energy surface of the reaction. It is of interest to determine whether similar effects are also important in intermolecular systems.

In the last few years, Weaver and co-workers[43-46] have carried out extensive studies on self-exchange intermolecular charge-transfer reactions in systems such as $Co[Cp]_2^0/Co[Cp]_2^+$ (Cp = cyclopentadienyl) using both electrochemical and NMR techniques. In polar aprotic solvents, the prefactors of the rate expression were found to correlate with the inverse of the longitudinal relaxation time of the liquid. Faster rates than those expected based on solvent relaxation data were found in alcohol solvents; the rate accelerations in these non-Debye solvents could be accounted for by using the faster relaxation components found in the frequency-dependent friction approach of Hynes and coworkers.[8] These workers stress throughout the studies that changes in the energetics of the reaction that result from changes in the solvent must be accounted for before any meaningful dynamic effects can be examined. This latter point is extremely important and plays an important role in determining the role of the solvent on the reaction rates reported in this paper.

Chart I

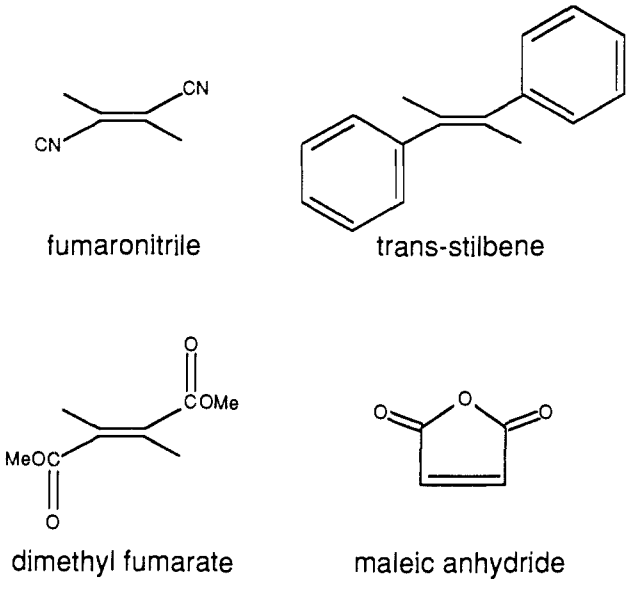

In the present study, the dynamics of an intermolecular charge-transfer reaction in polar aprotic solvents are examined. The reactions between the radical cation of *trans*-stilbene (TS) and the radical anion of fumaronitrile (FN), dimethyl fumarate (DF), and maleic anhydride (MA) have been well characterized by several workers.[47-51] The structures of the electron donor and acceptors are given in Chart I.

These chemical systems afford the advantage that contributions of diffusion to the reaction process are reduced; the ionic reactants are photogenerated by directly exciting a ground-state equilibrium complex between the two molecules. Thus, the dynamics examined involve a reaction between two ionic species, generating a neutral pair. In addition, in polar solvent, the most stable form of the photogenerated ions is free ions; thus, we would expect that the originally generated contact ion pair would also undergo diffusive separation. When the population decay of the photogenerated ions is examined, both the electron-transfer rate and the ion-pair separation process are quantified. Photolysis of the ground-state complex generates a species that, in many ways, is similar to a variety of intramolecular systems that have been studied. The role of solvation on this reaction process is discussed and compared to results obtained on intramolecular systems. Our results demonstrate that many of the insights that have been obtained from studies on intramolecular systems can be directly applied to intermolecular reaction dynamics.

Experimental Section

The picosecond absorption spectrometer has previously been described in detail.[52] Modifications include replacement of the standing dye

(23) Calef, D. F.; Wolynes, P. G. *J. Phys. Chem.* **1983**, *87*, 3387.
(24) Hynes, J. T. *J. Phys. Chem.* **1986**, *90*, 3701.
(25) Fonseca, T. *J. Chem. Phys.* **1989**, *91*, 2869.
(26) Gochev, A.; McManis, G. E.; Weaver, M. J. *J. Chem. Phys.* **1989**, *91*, 906.
(27) Zusman, L. D. *Chem. Phys.* **1980**, *49*, 295.
(28) Sparpaglione, M.; Mukamel, S. *J. Chem. Phys.* **1988**, *88*, 1465.
(29) Sparpaglione, M.; Mukamel, S. *J. Chem. Phys.* **1988**, *88*, 3263.
(30) Rips, I.; Jortner, J. *J. Chem. Phys.* **1987**, *87*, 2090.
(31) Rips, I.; Jortner, J. *J. Chem. Phys.* **1987**, *87*, 6513.
(32) Sumi, H.; Marcus, R. A. *J. Chem. Phys.* **1986**, *84*, 4272.
(33) Nadler, W.; Marcus, R. A. *J. Chem. Phys.* **1987**, *86*, 1906.
(34) Morillo, M.; Cukier, R. I. *J. Chem. Phys.* **1988**, *89*, 6736.
(35) Friedman, H. L.; Newton, M. *Faraday Discuss. Chem. Soc.* **1982**, *74*, 73.
(36) Maroncelli, M.; Fleming, G. R. *J. Chem. Phys.* **1987**, *86*, 1090.
(37) Su, S-G.; Simon, J. D. *J. Phys. Chem.* **1987**, *91*, 2693.
(38) Kahlow, M. A.; Jarzeba, W.; Kang, T-J.; Barbara, B. F. *J. Chem. Phys.* **1989**, *90*, 151.
(39) For a recent review see: Lippert, E.; Rettig, W.; Bonacic-Koutecky, V.; Heisel, F.; Miehe, J. A. *Adv. Chem. Phys.* **1987**, *68*, 1.
(40) Hicks, J.; Vabdersall, M. T.; Babarogic Z.; Eisenthal, K. B. *Chem. Phys. Lett.* **1985**, *116*, 18.
(41) Hicks, J.; Vandersall, M. T.; Sitzman, E.; Eisenthal, K. B. *Chem. Phys. Lett.* **1987**, *135*, 413.
(42) Simon, J. D.; Su, S-G. *J. Chem. Phys.*, in press.
(43) Weaver, M. J.; Gennett, T. *Chem. Phys. Lett.* **1985**, *113*, 213.
(44) Gennett, T.; Milner, D. F.; Weaver, M. J. *J. Phys. Chem.* **1985**, *89*, 2787.
(45) McManis, G. E.; Golovin, M. N.; Weaver, M. J. *J. Phys. Chem.* **1986**, *90*, 6563.
(46) Nielson, R. M.; McManis, G. E.; Golovin, M. N.; Weaver, M. J. *J. Phys. Chem.* **1988**, *92*, 3441.
(47) Angel, S. A.; Peters, K. S. *J. Phys. Chem.* **1989**, *93*, 713.
(48) Goodman, J. L.; Peters, K. S. *J. Am. Chem. Soc.* **1985**, *107*, 144.
(49) Goodman, J. L.; Peters, K. S. *J. Am. Chem. Soc.* **1985**, *107*, 6459.
(50) Goodman, J. L.; Peters, K. S. *J. Phys. Chem.* **1986**, *90*, 5506.
(51) Lewis, F. D. *Acc. Chem. Res.* **1979**, *12*, 152.
(52) Simon, J. D.; Peters, K. S. *J. Am. Chem. Soc.* **1983**, *105*, 4875.

solution with a flowing dye cell and the addition of an active 50-MHz mode-locking crystal (Interaction). Actively mode-locking the cavity increases the pulse to pulse stability but also decreases the energy of each pulse. This laser outputs a train of 10–15 pulses, each 30 ps wide at a repetition rate of 10 Hz with an average power of 10 mW. A single pulse is electrooptically extracted from the train and amplified. The rejected pulses are monitored by a storage scope that is used to trigger the detection electronics.

The amplified infrared pulse is used to generate both pump and probe laser beams. With two non-linear KDP crystals, light at 530 and 355 nm is generated. The UV light is separated from the 530-nm and residual 1060-nm light by a dichroic beam splitter. The UV light serves as the excitation beam and is passed through a computer-controlled shutter before being focused into the 1-cm path length sample cell. Both the 1060- and 530-nm pulses are focused into a continuum generating cell. The cell contains a 1:1 mixture of H_2O/D_2O and produces light from 400 to 600 nm.

The absorbance of the transient generated by the excitation pulse is monitored with a narrow spectral distribution selected from the continuum beam by a band-pass filter. Time resolution is obtained by varying the path length of the probe beam relative to the pump beam. Time $t = 0$ is defined as when the pump and probe beam have the same path length. The delay stage is 1.8 m in length and gives a maximum delay of just under 12 ns. A beam splitter is used to generate the I and I_0 beams needed for recording transient absorption signals. The reference beam (I_0) is focused onto a photodiode (E.G.G. DT110). The I beam is focused through the sample cell such that the pump and probe beams are collinear throughout the length of the cell. After the cell, any residual pump beam is filtered out and the probe beam is detected by a photodiode (E.G.G. DT110).

Analog signals from the photodiodes are passed to boxcar integrators (SRS 250) that are triggered by the storage scope. The boxcar integrates the signal and outputs a voltage that represents the area of the photodiode pulse. This signal is sent to a 12-bit analog to digital converter that is controlled by an IBM PC-XT. For each position of the delay stage, between 200 and 500 (depending on the noise level), laser shots are averaged to give I and I_0 without excitation (shutter is closed so that the pump beam is blocked) and I and I_0 with excitation (shutter opened). Only laser pulses within a preselected energy range are averaged. The transient absorbance is calculated by

$$\text{Abs} = \log\left(\frac{I_0}{I}\right)_{\text{with excitation}} - \log\left(\frac{I_0}{I}\right)_{\text{without excitation}} \quad (3)$$

The variance for each absorbance is also calculated and is at most 5% of the maximum absorption signal.

The above laser system is also used to record transient absorption spectra. In this case, the entire continuum is used for both the I and I_0 beams. The probe and reference beams are focused onto a 50-μm slit of a spectrograph that disperses the light onto the face of a ISIT vidicon detection system. The transient absorbance is calculated in the same manner as that used in carrying out single-wavelength studies.

Sample temperature is varied by flowing a temperature-controlled mixture of water and ethylene glycol through a jacketed 1-cm path length cell. The temperature inside the cell is measured with a thermocouple.

All samples studied were 0.025 M *trans*-stilbene and 0.125 M olefin. *trans*-Stilbene was recrystallized from ethanol, fumaronitrile was sublimed, dimethyl fumarate was recrystallized from water, and maleic anhydride was used with no further purification. Spectrograde acetonitrile was used with no further purification. The remaining nitrile solvents were stored over molecular sieves and distilled and/or passed over alumina just prior to use. All compounds were obtained from Aldrich.

The polarity of the solvent was determined by measuring the absorption maximum of Reichardt's dye (Aldrich). This scale, commonly referred to as the $E_T(30)$ parameter,[53] reflects the effect of the solvent on a transition between an ion-pair state and a neutral state. The $E_T(30)$ value is determined from the absorption spectrum of the dye in the solvent of interest with the following equation.

$$E_T(30) = \frac{2.86 \times 10^4}{\lambda_{max}\ (\text{nm})}\ (\text{kcal/mol}) \quad (4)$$

Results

In polar solvents, *trans*-stilbene and electron-poor olefins such as fumaronitrile, dimethyl fumarate, and maleic anhydride form stable ground-state complexes. This can be directly observed by

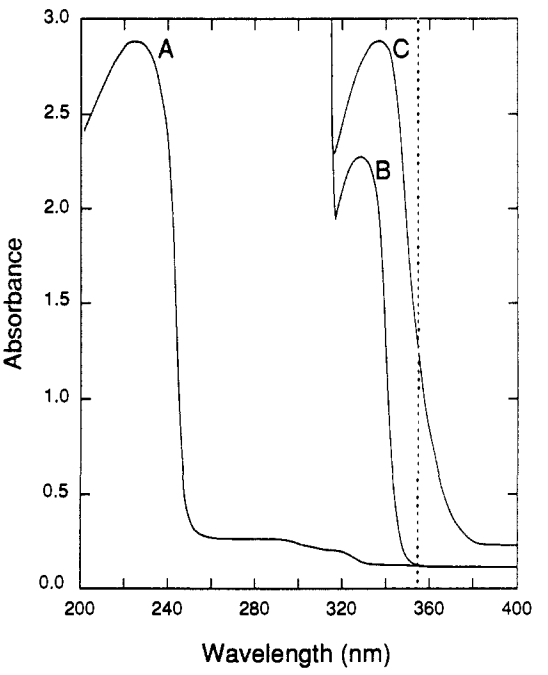

Figure 1. UV–vis absorption spectra of 0.125 M fumaronitrile (A), 0.025 M *trans*-stilbene (B), and a solution of 0.125 M fumaronitrile and 0.025 M *trans*-stilbene (C) in acetonitrile. The new absorption feature at ≈355 nm arises from a ground-state donor–acceptor complex between *trans*-stilbene and the electron-deficient olefin.

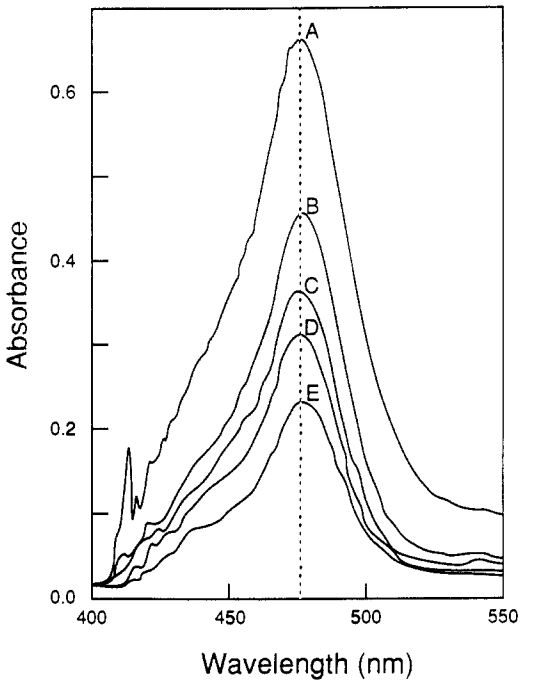

Figure 2. Transient absorption spectra observed following the photolysis of 0.025 M *trans*-stilbene and 0.125 M fumaronitrile in acetonitrile. The transient is assigned to the *trans*-stilbene radical cation. Delay time: 5 (A), 153 (B), 250 (C), 352 (D), and 650 (E) ps.

the appearance of a new absorption band that is red shifted from the first absorption feature of *trans*-stilbene (see Figure 1). With use of the approach of Benesi and Hilderband,[54] the equilibrium constant for formation of the ground-state complex between *trans*-stilbene and fumaronitrile,[47] dimethyl fumarate,[55] and maleic anhydride[56] can be determined and has been reported to be 0.13,

(53) Reichardt, C. *Solvent Effects in Organic Chemistry*; Verlag-Chemie: Weinheim, 1978; and references therein.

(54) Benesi, H. A.; Hildebrand, J. H. *J. Am. Chem. Soc.* **1949**, *71*, 2703.
(55) Green, B. S.; Rejto, M.; Johnson, D. E.; Hoyle, C. E.; Ho, T. I.; McCoy, F.; Simp, J. T.; Lewis, F. D. *J. Am. Chem. Soc.* **1979**, *101*, 3325.
(56) Rzayev, Z. M.; Zeinalov, I. P.; Medyakova, L. V.; Babayev, A. I.; Agayev, M. M. *Vysokomol. Soedin, Ser. A* **1981**, *23*, 614.

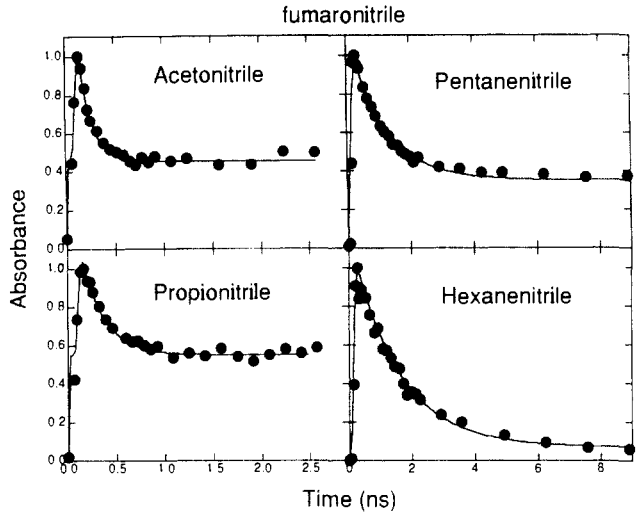

Figure 3. Transient absorption signal at 475 nm plotted as a function of time following the photolysis of the *trans*-stilbene/fumaronitrile complex in various nitrile solvents. The data reflect the decay of the photogenerated *trans*-stilbene radical cation. The rate of decay (see text) decreases with increasing chain length (note the different time scales for the various solvents studied). The solid line is a fit of the kinetic model discussed in the text. The data have been normalized for ease of comparison. The maximum signals observed are $A \approx 0.3$.

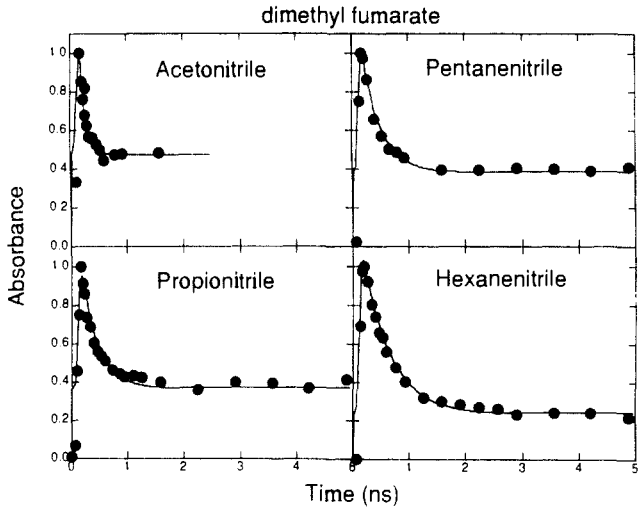

Figure 4. Transient absorption signal at 475 nm plotted as a function of time following the photolysis of the *trans*-stilbene/dimethyl fumarate complex in various nitrile solvents. The data reflect the decay of photogenerated *trans*-stilbene radical cation. The rate of decay (see text) decreases with increasing chain length. The solid line is a fit of the kinetic model discussed in the text. The data have been normalized for ease of comparison. The maximum signals observed are $A \approx 0.3$.

1.0, and 0.21 M^{-1}, respectively. Examining the spectra in Figure 1, we see that in a solution of 0.025 M *trans*-stilbene and 0.125 M olefin irradiating at 355 nm only excites the ground-state complex. The results of photolysis in acetonitrile at this wavelength are shown in Figure 2. Excitation generates a visibly absorbing intermediate with a λ_{max} of 475 nm within the laser pulse. The transient absorbance at 475 nm decreases with time; however, the spectral shape of the band remains constant. This transient absorption spectrum is identical with that of the *trans*-stilbene radical cation.[57] The transient absorption dynamics observed at 475 nm following photolysis of TS/FN in acetonitrile, propionitrile, butyronitrile, pentanenitrile, and hexanenitrile are shown in Figure 3. Similar spectra for the TS/DF and TS/MA are shown in Figures 4 and 5, respectively. In all cases, the transient signal

(57) Hamil, W. H. In *Radical Ions*; Kaiser, E. T., Kevan, T., Eds.; Wiley: New York, 1968.

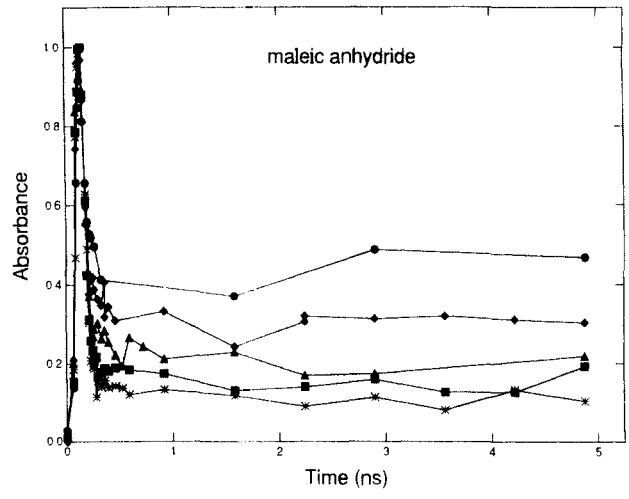

Figure 5. Transient absorption signal at 475 nm plotted as a function of time following the photolysis of the *trans*-stilbene/maleic anhydride complex in various nitrile solvents. The data reflect the decay of photogenerated *trans*-stilbene radical cation. The initial rate is limited by the time resolution of the experiment. The solvents plotted are acetonitrile (●), propionitrile (◆), pentanenitrile (■), and hexanenitrile (*).

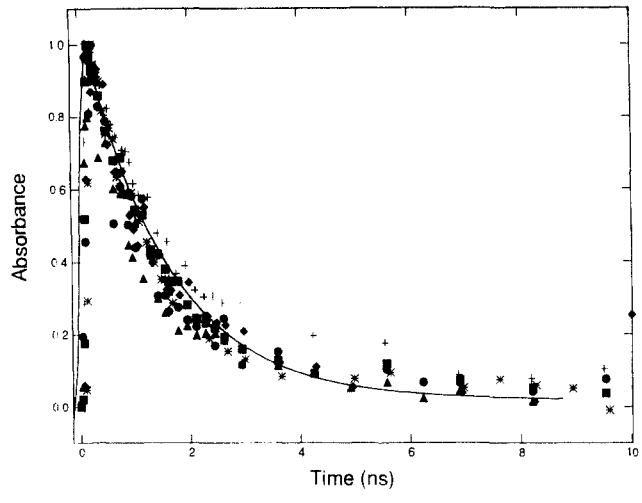

Figure 6. Transient absorption signal at 475 nm plotted as a function of time following the photolysis of the *trans*-stilbene/fumaronitrile complex in hexanenitrile at various temperatures: −8 (■), 6.5 (*), 25 (+), 30 (●), 50 (▲), 80 (◆) °C. These data show that the dynamics are temperature-independent over the range studied. Similar results are observed in all the nitrile solvents examined.

exhibits a fast-decay component followed by an essentially constant absorption at long delay times. As the polarity of the solvent is decreased, the initial rate of decay of the radical cation decreases and the time at which the transient signal becomes constant increases. In the reaction between $TS^{\bullet+}$ and $MA^{\bullet-}$, both the rate of electron transfer and the rate of ion-pair separation are faster than our instrument response ($>3 \times 10^{10}$ s^{-1}).

In Figure 6, the decay of the *trans*-stilbene radical cation formed by photolysis of the TS/FN ground-state complex is examined in hexanenitrile as a function of temperature. Within the signal to noise of the experiment, there is no temperature dependence of the absorption dynamics. Similar temperature-independent data are observed in the entire series of linear nitrile solvents for all three olefins studied.

Discussion

Following excitation of the ground-state charge-transfer complex (CTC) between *trans*-stilbene and an electron-poor olefin, a contact ion pair (CIP) between the radical cation of *trans*-stilbene and the radical anion of the olefin is generated. This species then either undergoes intermolecular charge transfer, re-forming the ground-state neutral pair, or separates to form free ions (FI).

Scheme I

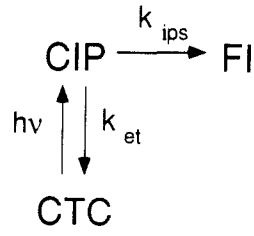

Several factors can influence the dynamics of charge transfer and ion-pair separation and, hence, the time-dependent concentration of the *trans*-stilbene radical cation. In polar solvents, the resulting ions will separate to form the more thermodynamically stable solvent-separated ion pair and freely solvated ions.[58] This diffusional process would compete with the electron back-transfer reaction. Thus, in principle, a time-dependent rate of electron transfer could be observed, reflecting the changes in equilibrium distances between the two reacting species. Unlike a variety of intermolecular charge-transfer systems that have been studied to date, the present system affords the advantage that the initial distribution of photogenerated reactants are in contact, eliminating the need for the ions to diffuse together in order to undergo electron transfer. As we will demonstrate in the following discussion, this important feature enables one to quantitatively determine the effects of the solvent on the energetics of the charge-transfer process.

A. Determination of the Rate Constants for Charge Transfer. As indicated earlier, excitation of the *trans*-stilbene/olefin ground-state complex at 355 nm generates contact ion pairs. In deriving rate constants from the time-dependent absorption signal of the *trans*-stilbene radical cation, we assume that the photogenerated ion pair undergoes two competing reactions: electron back-transfer (k_{et}) and ion-pair separation (k_{ips}) (Scheme I).

As previously suggested, one might expect a time-dependent rate constant for the electron-transfer rate, reflecting charge back-transfer from reactant species at a variety of intermolecular distances.[17] However, careful examination of the data suggests that this is not the case. In all solutions studied, the transient signal decreases to a constant absorbance that lasts for at least 12 ns (the limit of our experimental delay line). This leads to two major conclusions. First, the separated ions do not diffuse back together to form contact ion pairs, which would then undergo electron back-transfer. Second, at whatever interionic distance is achieved within the first few nanoseconds, the rate of electron back-transfer is negligible. According to Siders and Marcus, the distance dependence of the electron-transfer rate can be expressed by[17]

$$k_{et} \propto \exp\{-\alpha(r - \sigma)\} \tag{5}$$

where r is the separation of the reactants and σ is their contact distance and α is an adjustable parameter. For a case where the reactants are separated by roughly one solvent shell (≈5 Å) and $\alpha = 1.5$ Å^{-1}, the rate decreases by a factor of 2000 from that calculated for ions in contact.[17] Assuming a codiffusion constant[47] of 3.2×10^{-5} cm^2/s, the minimum time required for the ions to separate 5 Å is approximately 40 ps. Therefore, it is unlikely that we are observing a distribution of electron-transfer rates that are dependent on the separation of the reactants. This conclusion is also consistent with a previous analysis of the forward intermolecular charge transfer between photoexcited *trans*-stilbene and fumaronitrile (not a direct excitation of the ground-state complex), where a careful analysis of the dynamics revealed that charge transfer occurred only after the reactants become cosolvated.[47]

The transient absorption reflects the total concentration of *trans*-stilbene radical cation, regardless of the ion-pair structure. When the kinetic analysis is carried out, it is assumed tht the only process that destroys this species is electron back-transfer.

(58) Smid, J. In *Ions and Ion Pairs in Organic Chemistry*; Szwarc, C. M., Ed.; Wiley: New York, 1974; Vol. 1.

Table I. Tabulation of the Rates of Electron Transfer (k_{et}) and Ion-Pair Separation (k_{ips}) (See Scheme I) at 298 K for the Reaction between the *trans*-Stilbene Radical Cation and the Radical Cations of Fumaronitrile and Dimethyl Fumarate[a,b]

	fumaronitrile		dimethyl fumarate	
solvent	k_{et}	k_{ips}	k_{et}	k_{ips}
acetonitrile	4.70	2.90	7.50	4.00
propionitrile	2.21	2.06	3.84	1.43
butyronitrile	1.30	1.19	2.63	0.91
pentanenitrile	1.01	0.40	2.61	0.90
hexanenitrile	0.66	0.089	1.75	0.04

[a] Rate constants are roughly ±10% for reaction with fumaronitrile and ±20% for dimethyl fumarate. The corresponding data with maleic anhydride are not tabulated as both rates are faster than our instrument response. [b] All rates are in units of 10^9 s^{-1}.

Furthermore, it is assumed that the extinction coefficient of the radical cation is insensitive to the ion-pair structure. This is consistent with the data shown in Figure 2. This figure demonstrates that the shape of the spectral transient is invariant with time. Assuming that the early-time spectra reflect radical cations in contact ion pairs and the long-time transient are freely solvated ions, the separation process has no effect on the transient spectrum. Under these conditions, the kinetics shown in Scheme I are easily solved. The time-dependent concentration of the radical cation of *trans*-stilbene is expressed as follows:

$$[TS^+](t) = C\left\{\left(1 - \frac{k_{ips}}{k_{et} + k_{ips}}\right)e^{-(k_{et}+k_{ips})t} + \frac{k_{ips}}{k_{et} + k_{ips}}\right\} \tag{6}$$

In the above equation, C is a constant that reflects the concentration of radical cation at t = 0. In order to compare with the experimental data ($A(t)$), this expression needs to be convolved with the response function of the instrument ($I(\tau)$) as expressed below.

$$A(t) = \int_{-\infty}^{t} I(\tau)\,[TS^+](t - \tau)\,d\tau \tag{7}$$

The instrument response function is determined by assuming a Gaussian pulse shape and fitting the rise of the $T_1 \rightarrow T_N$ absorption of benzophenone (assumed to be instantaneous[59]). The values of k_{et} and k_{ips} are determined by a convolution and compare algorithm that minimizes the deviations between the calculated curves and the experimental data. The resulting rate constants are given in Table I.

B. Solvent and Temperature Dependence of k_{et}. The observation that k_{et} is temperature-independent might lead one to conclude that the process either is activationless or is controlled by quantum mechanical tunneling. In the following discussion, we suggest a model in which the activation barrier is temperature-dependent and can be parameterized in terms of the temperature dependence of the dielectric properties of the reaction medium.

The data in Table I indicate that the rate constant for electron back-transfer is solvent-dependent, with decreasing rates observed with decreasing polarity. However, one would also expect that, with decreasing polarity, the ion-pair state is destablized with respect to the ground state and the exoergicity of the electron back-transfer would increase.[51]

In the standard Marcus model of electron transfer, the dominant contribution of the solvent is to alter the overall free energy, resulting in a change in reaction rate. The free energy relationship given by eq 2 indicates that such a change would affect the magnitude of the activation energy for reaction.

Using the reported[60] oxidation potential for *trans*-stilbene in acetonitrile of 1.5 eV and reduction potentials for fumaronitrile,[60]

(59) The intersystem crossing rate for benzophenone following excitation is $1/k_{ips} < 5$ ps. The dynamics of this process have no effect on the instrument response function derived assuming a δ function as the laser pulse width is significantly longer than the intersystem crossing rate.

(60) Lewis, F. D. *Adv. Photochem.* **1986**, *13*, 165.

Table II. Tabulation of the Exoergicites and Activation Parameters for the Electron-Transfer Reaction between the *trans*-Stilbene Radical Cation and the Anion of Fumaronitrile and Dimethyl Fumarate[a,b]

		fumaronitrile				dimethyl fumarate			
solvent	τ_s	A	ΔG_0	$\Delta G^{\ddagger}$	ΔG°	A	ΔG_0	$\Delta G^{\ddagger}$	ΔG°
acetonitrile	0.7	3.32	65.78	2.54	7.04	1.67	69.92	1.85	5.13
propionitrile	1.1	0.79	66.28	2.13	5.97	0.52	70.42	1.55	4.35
butyronitrile	1.6	0.44	66.66	2.10	5.66	0.34	70.80	1.53	4.13
pentanenitrile	c	0.55	67.08	2.38	5.82	0.48	71.22	1.73	4.24
hexanenitrile	c	1.49	67.46	3.23	6.65	0.91	71.60	2.35	4.85

[a] Activation parameters are derived with the solvent polarity correction described in the text. [b] Units: free energies, kcal/mol; prefactors, 10^{-11} s^{-1}; τ_s, ps. [c] Also tabulated are the solvent relaxation times from studies of coumarin 311. No data available for coumarin 311.

dimethyl fumarate,[61] and maleic anhydride[60] in acetonitrile of −1.36, −1.56, and −0.84 eV, respectively, the exoergicity of the electron back-transfer reaction can be calculated with the following expression.

$$\Delta G_0 = E(\mathrm{D}/\mathrm{D}^+) + E(\mathrm{A}/\mathrm{A}^-) - \frac{e^2}{\epsilon r_{\mathrm{DA}}} \qquad (8)$$

The last term, which accounts for the Coulombic attraction between the two ions, is difficult to determine. Theoretical calculations[62] using a molecular model for the solvent clearly demonstrate that the local dielectric constant in the vicinity of an ion is reduced from the bulk value. In this limit, the value of $e^2/\epsilon r$ is small and will be nearly constant for the series of solvents studied. Omitting this contribution, ΔG_0 is −66, −70, and −54 kcal/mol for ion pairs of *trans*-stilbene and FN, DF, and MA in acetonitrile, respectively. With use of a Born correction term to quantify changes in the solvation energy of the two ions,[63] changes in the electrochemical values relative to acetonitrile in the various solvents studied can be determined:

$$E_{\mathrm{D}}^{\mathrm{ox}} + E_{\mathrm{A}}^{\mathrm{red}} = (E_{\mathrm{D}}^{\mathrm{ox}} + E_{\mathrm{A}}^{\mathrm{red}})_{37.5} + \frac{e^2}{2}\left(\frac{1}{r_-} + \frac{1}{r_+}\right)\left(\frac{1}{\epsilon_s} - \frac{1}{37.5}\right) \qquad (9)$$

Using this approach, we find that the reaction between $TS^{\bullet+}$ and $FN^{\bullet-}$ becomes more exoergic by 1.5 kcal/mol when the solvent is changed from acetonitrile to hexanenitrile. The rate constants given in Table I show a decrease in rate with an increase in exoergicity, a behavior characteristic of the Marcus inverted region. Observation of the Marcus inverted region implies that there is a reaction barrier (eq 2). This conclusion contradicts the temperature independence of the rate (see Figure 6) that implies no barrier to reaction.

Varying the solvent changes the polarity of the reaction medium, affecting the energetics and rate of the reaction. Along these lines, Eisenthal and co-workers developed a model to account for polarity effects on the activation barrier in order to determine the importance of solvent viscosity on the intramolecular charge-transfer dynamics of (*N*,*N*-dimethylamino)benzonitrile in long-chain nitrile solvents.[10] In this model, the activation energy is expressed in terms of an intrinsic barrier (ΔG°) (that expected in a hydrocarbon solvent, $E_T(30) = 30$) and a contribution that is linearly dependent on solvent polarity.

$$\Delta G^{\ddagger} = \Delta G^{\circ} + \alpha(E_T(30) - 30) \qquad (10)$$

This expression indicates that the logarithm of the reaction rate should be linear with the $E_T(30)$ value of the solvent, as found in Figure 7. From the data given in this figure, the value of α is determined to be −0.28 and −0.20 for FN and DF, respectively.

In addition, in any given solvent, an increase in temperature results in a decrease in solvent polarity,[51] causing a decrease in the electron-transfer rate for reactions in the Marcus inverted region. However, under normal Arrhenius considerations, an increase in temperature is also expected to increase the magnitude of the rate constant. These two effects oppose each other. When the approach developed by Eisenthal is carried out, polarity effects on the reaction barrier resulting from the solution temperature need to be accounted for. In Table IV, the temperature dependence of the $E_T(30)$ values for the various solvents studied are given. In all cases, a linear dependence of the $E_T(30)$ value with temperature is observed. This is consistent with previous reports for alcohol solvents.[53] Within this model, the activation energy for the electron-transfer reaction, eq 10, can be written as

$$\Delta G^{\ddagger} = \Delta G^{\circ} + \alpha(\gamma + \delta T) \qquad (11)$$

where γ is value of $E_T(30) - 30$ at 0 K and δ is the temperature dependence of the solvent polarity ($d(E_T(30) - 30)/dT$). The right-hand side of this equation can be divided into a temperature-dependent and temperature-independent term:

$$\frac{\Delta G^{\ddagger}}{RT} = \left(\frac{\Delta G^{\circ} + \alpha\gamma}{RT} + \frac{\alpha\delta}{R}\right) \qquad (12)$$

The reaction rate depends exponentially on eq 12. If the temperature-dependent term is much smaller than the temperature-independent term for the temperature range examined (i.e., $\Delta G^{\circ} \approx -\alpha\gamma$), the above expression would predict that the observed dynamics would be temperature-independent. The three constants, α, γ, and δ, are independently determined, and the temperature independence of the reaction gives $\Delta G^{\circ} = -\alpha\gamma$. Using the data shown in Figure 7 and Table IV, we find that $\Delta G^{\circ} = 6.2 \pm 0.7$ and 4.5 ± 0.6 kcal/mol for FN for DF, respectively. The prefactor can be determined for all the systems studied from the room-temperature rate and polarity data and for the series of solvents

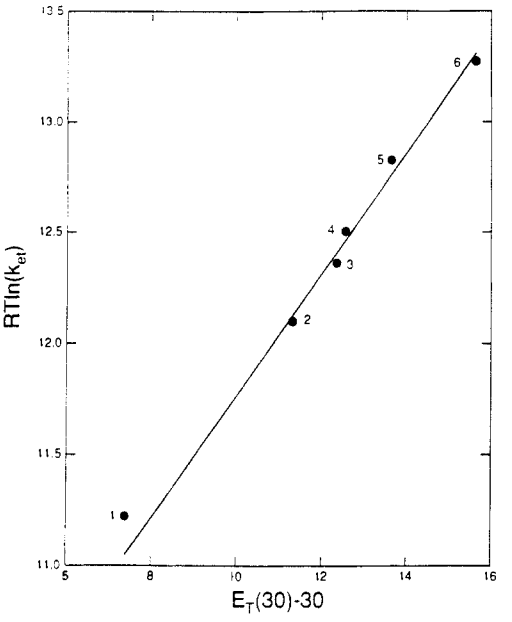

Figure 7. Log of the rate constant (ln k_{et}) for reaction between the radical cation of *trans*-stilbene and the radical anion of fumaronitrile plotted as a function of solvent polarity ($E_T(30) - 30$). Solvents used are THF (1), hexanenitrile (2), pentanenitrile (3), butyronitrile (4), propionitrile (5), and acetonitrile (6).

(61) Sazou, D.; Karabinas, P. *Collect. Czech. Chem. Commun.* **1987**, *52*, 2132.
(62) Morita, T.; Ladanyi, B. M.; Hynes, J. T. *J. Phys. Chem.* **1989**, *93*, 1386.
(63) Born, M. *Z. Physik.* **1920**, *1*, 45.

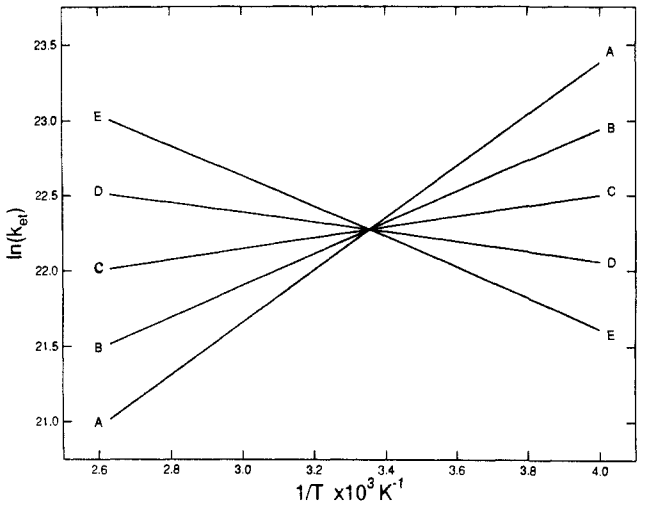

Figure 8. Temperature dependence of ln k_{et} plotted for various values of the intrinsic barrier ($\Delta G°$): 3.4 (A), 4.8 (B), 6.2 (C), 7.6 (D), 9.0 (E) kcal/mol. The intercept from Figure 8 is used to calculate A. The calculation shows that for various values of $\Delta G°$ k_{et} can exhibit Arrhenius behavior, no temperature dependence, or non-Arrhenius dynamics.

studies. These values range from 0.45 to 3.3 × 10^{11} s^{-1} for FN and from 0.34 to 1.7 × 10^{11} s^{-1} for DF; see Table II.

If $\Delta G° \neq -\alpha\gamma$, there are two unknowns in determining k_{et}, $\Delta G°$ and A. However, the plot of RT ln k_{et} as a function of $E_T(30)$ shown in Figure 7 gives the y intercept of RT ln $A - \Delta G°$, leaving only one adjustable parameter. In Figure 8, the temperature dependence of k_{et} for the reaction between $TS^{\bullet+}$ and $FN^{\bullet-}$ is plotted assuming various values for the intrinsic barrier ($\Delta G°$) (and using the y intercept from Figure 7 to determine A). For an intrinsic barrier of 3.5 kcal/mol, k_{et} decreases with increasing temperature, while for an intrinsic barrier of 9.0 kcal/mol k_{et} increases with increasing temperature. However, for $\Delta G° \approx 7.0$ kcal/mol, no temperature dependence is calculated. Rigorously, the prefactor (A) is also temperature dependent; however, over the temperature range studied, this effect is small compared to the above calculations involving $\Delta G^{\ddagger}$.

Based on several theoretical descriptions of charge-transfer reactions, the effects of solvent dynamics on the reaction rate should be manifested in the prefactor (A).[43-46] In general, an inverse relationship between the solvent relaxation time, τ_s, and the prefactor is expected. Correlations between A and solvent relaxation times have been observed for several intramolecular systems.[11,64,65] McGuire and McLendon[66] and Weaver and co-workers[8,43-46] have also reported similar correlations for a variety of intermolecular systems. Recently, relaxation times have been experimentally determined from time-resolved Stokes shift measurements for several of the nitrile solvents.[1-5,67] These are also listed in Table II. Qualitatively, for the series of short-chain nitrile solvents (acetonitrile–butyronitrile), the magnitude of the prefactor decreases with increasing solvent relaxation time. It is interesting to note that for the first three solvents in the nitrile series for both reaction with the radical anions of fumaronitrile and dimethyl fumarate, a good correlation is observed between the A value and the inverse of the solvent relaxation time. However, for the longer chain solvent, i.e., pentanenitrile and hexanenitrile, an increase in the magnitude of the prefactor is observed. Unfortunately, a quantitative analysis cannot be carried out. In the longer chain nitriles, multiple components are observed in the solvent relaxation studies[4] and the relative importance of these different solvent relaxation times in determining the magnitude of the prefactor are not known. Barbara and Weaver and co-workers[8] have recently suggested that in non-Debye fluids the fast-relaxation components can have a significant effect on the rate of charge transfer. With increasing chain length, the series of nitrile solvents exhibit more complicated time-dependent Stoke shift decays, and hence reflect the presence of a wider distribution of relaxation times. The observed dependence of the prefactor in the electron-transfer reactions between the stilbene radical cation and the olefin radical anions might reflect the importance of fast solvation processes in the long-chain nitrile solvents. More detailed solvation measurements are needed to address this issue.

For each individual olefin studied, the dependence of k_{et} on $\Delta G°$ was consistent with the predictions of the Marcus inverted region. However, when the different acceptors are compared, the rate of electron transfer for DF is faster than FN even though the reaction with DF is more exoergic. In addition, for each olefin, the reaction rate constant correlates linearly with solvent dielectric constant. If energetics were the only important factor in determining the reaction rate, one could use eq 9 and 10 and the experimental data for the TS/FN system to predict the rate constant for a solvent in which the reaction exoergicity would be −70 kcal/mol, the exoergicity of the $TS^{\bullet+}/DF^{\bullet-}$ reaction in acetonitrile. Such a calculation predicts a k_{et} of 3.4 × 10^8, significantly different from that observed of 7.5 × 10^9. This result demonstrates that other factors are important in determining the rate of electron transfer. Furthermore, these results show that one cannot assume that by simply varying the electron acceptor (or donor) the resulting rate data reflects an accurate measure of the dependence of electron-transfer rates on reaction exoergicity and can be used as a test of the Marcus free energy relationship. The three olefins chosen for the present study are very similar, but the results clearly show that these systems cannot be used to map out the Marcus free energy curve. The TS/FN and TS/DF systems have very similar prefactors and solvent contributions to the reorganization energy (see section C) (λ_s); the most significant difference is that within the model described above the intrinsic barrier ($\Delta G°$) varies for the different olefins studied.

Table III. Tabulation of the Reorganization Energy (λ) (Eq 14) by Use of the Polarity-Corrected Values in Table II[a,b]

		fumaronitrile		dimethyl fumarate	
solvent	λ_s	λ	λ_i	λ	λ_i
acetonitrile	1.03	1.94	0.91	2.20	1.17
propionitrile	1.02	2.02	1.00	2.28	1.26
butyronitrile	1.00	2.04	1.04	2.30	1.30
pentanenitrile	1.00	2.01	1.01	2.27	1.27
hexanenitrile	1.00	1.90	0.90	2.17	1.17

[a] Eq 13 is used to determine λ_s, from which the inner-sphere contribution (λ_i) can be calculated from $\lambda_i = \lambda - \lambda_s$. [b] All organization energies are in units of eV.

C. Evaluation of the Reorganization Energy. From the above analysis, the energetics (both exoergicity and activation energies) of the electron-transfer reaction between the radical cation of *trans*-stilbene and the radical anion of fumaronitrile can be determined. With this information, it is possible to quantify the reorganization energy (λ). In general, various factors contribute to the magnitude of λ. Contributions arise from both the solvent (λ_s) and internal modes (λ_i). The former is generally described in terms of the following expression[68,69] modeling the solvent as a dielectric continuum.

$$\lambda_s = -e^2\left(\frac{1}{2r_D} + \frac{1}{2r_A} - \frac{1}{r_{DA}}\right)\left(\frac{1}{\epsilon_s} - \frac{1}{n_s^2}\right) \qquad (13)$$

In the above expression r_D, r_A, and r_{DA} are the radii of the donor and acceptor and intermolecular distance, respectively. λ_i is a function of the changes in vibrational frequencies and bond lengths that occur with product formation. From the free energy rela-

(64) Simon, J. D.; Su, S-G. *J. Phys. Chem.* **1988**, *92*, 2395.
(65) Kosower, E. M.; Huppert, D. *Ann. Rev. Phys. Chem.* **1986**, *37*, 127, and references therein.
(66) McGuire, M.; McLendon, G. *J. Phys. Chem.* **1986**, *90*, 2549.
(67) Barbara, P. F. Personal communication.
(68) Marcus, R. A. *J. Chem. Phys.* **1965**, *43*, 679.
(69) Hush, H. S. *Prog. Inorg. Chem.* **1967**, *8*, 391.

tionship given in eq 2 and the activation energies and exoergicities tabulated in Table II, the value of λ ($\lambda = \lambda_s + \lambda_i$) can be determined with use of the following expression.

$$\lambda = \tfrac{1}{2}[(4\Delta G^{\ddagger} - 2\Delta G_0) \pm [(2\Delta G_0 - 4\Delta G^{\ddagger})^2 - 4\Delta G_0^2]^{1/2}] \quad (14)$$

The results are tabulated in Table III. For the series of nitrile solvents, the value of λ is essentially constant, being approximately 2 eV. From eq 13, the contribution of static solvent effects to the reorganization energy can be determined. These values, also tabulated in Table III, account for approximately half of the total energy. When this calculation was carried out, r_D and r_A were determined from van der Waal radii[70] and found to be 8 and 5 Å, respectively. The internuclear distance (r_{DA}) was set to 3.5 Å, as previously reported by Lewis and co-workers.[60] We conclude from this analysis that there is a significant contribution from the internal modes of the system to the reorganization energy. With the expected changes in vibrational frequencies between the neutral molecules and the respective ions, a large inner-sphere contribution to λ is anticipated. It is important to point out that the determination of λ is only possible after the reaction rates are corrected for polarity as described in the previous section.

These results of $\lambda \approx 2.0$ eV are similar to those from studies of both inter- and intramolecular electron transfer where λ is determined by fitting ln k_{et} as a function of ΔG_0 to a parabola (eqs 1 and 2).[5,22] For example, intermolecular electron-transfer reactions between substituted anthracenes and a series of donors[71] yielded λ = 1.7–1.9 eV.

D. Dynamics of Ion-Pair Separation. The presence of a constant absorption for the *trans*-stilbene radical cation at long delay times indicates that a fraction of the initially formed contact ion pairs separate to form stable free ions. On the basis of extensive studies of ion-pair dynamics in polar fluids, this separation process is thought to involve several kinetically stable intermediates, corresponding to different degrees of solvation. Unfortunately, the spectroscopy of the system studied in this paper does not lend itself to examine the role of intermediate species such as the solent-separated ion pair. From the time-dependent decays, it is known that, once separated, the rate of reformation of the contact ion pair is very slow. If this were not the case, the signal observed at long delay times would continue to decrease, reflecting electron back-transfer. The observation of a constant signal indicates that the thermodynamic equilibrium lies strongly in favor of separated ions. However, as shown in Figure 2, the spectrum of the radical cation is not sensitive to changes in the ion-pair structure. Thus, it cannot be used to probe the molecular dynamics associated with ion-pair separation. As a result, it is unclear whether k_{ips} represents the rate of a single process or a convolution of many kinetic events.

On the basis of the kinetic model developed in this paper, we find that the separation process, as defined by k_{ips}, is essentially temperature-independent. In this case, one would conclude that the enthalpy for ion-pair separation is less than 1 kcal/mol. Assuming a barrier of this magnitude, a preexponential factor of 10^8 s^{-1} is needed to account for the observed dynamics. By use of activated complex theory,[72] this suggests an activation entropy of −15 cal/(K mol). Although we cannot ascribe a molecular process to k_{ips}, these results suggest that the ion-pair separation is entropically controlled. Similar activation energies have been observed for inorganic ion pairs. For example, NMR studies of the formation dynamics of free ions from contact ion pairs[73] of $Me_3PCO_3NOW^+SbF_6^-$ and related molecules in hexane find an activation entropy and enthalpy of −19 cal/(K mol) and 2 kcal/mol, respectively.

Table IV

solvent	$E_T(30)$ at 298 K	$d[E_T(30) - 30]/dT$
THF	37.8	−0.024
chloroform	39.5	−0.030
dichloromethane	41.5	−0.053
acetonitrile	46.6	−0.031
propionitrile	44.0	−0.026
butyronitrile	43.1	−0.026
pentanenitrile	42.6	−0.029
hexanenitrile	42.5	−0.040
propanol	50.4	0.037
butanol	49.6	−0.042
pentanol	49.3	−0.041
hexanol	49.1	−0.033

Acknowledgment. K.S.P. and J.D.S. acknowledge support from the National Science Foundation. We thank Professor James T. Hynes for many helpful discussions and his hospitality during the sabbatical stay of J.D.S.

Appendix

The temperature dependence of $E_T(30)$ was measured for a series of solvents. A linear correlation was observed between $E_T(30) - 30$ and temperature. Results are tabulated in Table IV.

(70) Bondi, A. *J. Phys. Chem.* **1964**, *68*, 441.
(71) Gould, I. R.; Moser, J. E.; Moody, R.; Armitage, B.; Farid, S. *J. Imaging Sci.* **1989**, *33*, 44.
(72) Glasstone; Laidler; Eyring. *The Theory of Rate Processes*; McGraw-Hill: New York, 1941.
(73) Honeychuch, R.; Hersh, W. H. *J. Am. Chem. Soc.* **1989**, *111*, 6056.